Electronic Supplementary Information

Experimental Section

Materials: Hydrochloric acid (HCl), sulfuric acid (H_2SO_4), potassium permanganate ($KMnO_4$), ethyl alcohol (C_2H_5OH), sodium carbonate (Na_2CO_3), and potassium hydroxide (KOH) were purchased from Chengdu Kelong Chemical Reagent Factory. Nickel chloride hexahydrate ($NiCl_2 \cdot 6H_2O$), cobalt chloride hexahydrate ($CoCl_2 \cdot 6H_2O$), ruthenium oxide (RuO_2), Pt/C (20% wt% Pt on Vulcan XC-72R), Nafion (5 wt%), ammonium chloride (NH_4Cl), and sodium hypophosphite (NaH_2PO_2) were provided by Aladdin Industrial Co. Ltd. N, N-diethyl-p-phenylenediamine (DPD) was achieved from Shanghai Maclin Biochemical Technology Co., Ltd. All the reagents and chemicals were used as received without further purification. The deionized water (resistivity: 18.3 MΩ·cm) used for all experiments was purified through a Millipore system. Natural seawater was obtained from Weihai, Shandong, China, and most of the magnesium and calcium salts were eliminated by adding 6.8 g Na_2CO_3 to 1 L of natural seawater before use. Ni foam (NF, thickness:1.5 mm, porosity: ≥ 95%) was bought from Shenzhen Green and Creative Environmental Science and Technology Co. Ltd.

Preparation of Ni-Co alloy foam/NF: Ni-Co alloy on NF was prepared by a one-step dynamic hydrogen bubble template method. Initially, a piece of NF (2×3 cm^2) was immersed into a 2 M HCl solution for 10 minutes to remove any potential surface oxide layer. Subsequently, the NF was alternately washed in ethanol and deionized water for 5 minutes each, using sonication to eliminate any residual chemical traces. The electrodynamic deposition was performed at room temperature using a three-electrode cell set-up. The working electrode with NF, the reference electrode (Ag/AgCl, saturated KCl),

and the counter electrode (graphite) were immersed in an electrolyte solution composed of 0.2 M $CoCl_2$, 0.05 M $NiCl_2 \cdot 6H_2O$, and 2.0 M NH_4Cl. The deposition process was carried out at a constant current of -2 A/cm^2 for 120 seconds at room temperature. After deposition, the prepared Ni-Co alloy foam/NF was thoroughly rinsed with deionized water and air-dried overnight.

Preparation of NiCoP foam/NF: A porcelain boat containing approximately 0.5 g of NaH_2PO_2, along with another porcelain boat holding a piece of the as-prepared Ni-Co alloy foam/NF, was positioned in the center of a tube furnace. It is important to place the NaH_2PO_2 on the upstream side of the furnace. Before initiating the heating process, argon gas flowed through the tube. The furnace temperature was then gradually increased to 300 °C at a rate of 2 °C/min and maintained at this temperature for 2 hours under an argon atmosphere. Following this, the system was allowed to cool down to room temperature, resulting in the formation of the NiCoP foam/NF.

Synthesis of Ni_2P and Co_2P foam/NF: The procedures for synthesizing Ni_2P and Co_2P foam/NF are similar to those used for NiCoP foam/NF, with a few key differences. Specifically, for Ni_2P foam /NF, the material is immersed in an electrolyte solution consisting of 0.05 M $NiCl_2 \cdot 6H_2O$, and 2.0 M NH_4Cl. In contrast, for Co_2P foam/NF, the immersion is in a solution of 0.2 M $CoCl_2$ and 2.0 M NH_4Cl. Following these immersion steps, both alloy foams undergo phosphidation under the same conditions as used for the NiCoP foam/NF.

Synthesis of RuO_2 or Pt/C on NF: 5 mg RuO_2 (or 20% Pt/C) was added to a mixture containing 30 µL of Nafion, 485 µL of ethanol, and 485 µL of deionized water. To ensure a homogenous dispersion, the solution was subjected to ultrasonication for 30 minutes,

resulting in a concentration of 5 mg/mL. Subsequently, 150 µL of this catalyst ink was carefully dropped onto a piece of cleaned NF (0.5 cm × 0.5 cm) with a loading mass of 0.75 mg.

Characterization: Scanning electron microscopy (SEM) images and energy-dispersive X-ray spectroscopic (EDX) analyses were performed on Zeiss Gemni SEM 300 at an accelerating voltage of 5 kV and Transmission electron microscopy (TEM) was carried out with a HITACHI H-8100 electron microscope (Hitachi, Tokyo, Japan) operated at 200 kV. The X-ray diffraction (XRD) patterns were conducted with a Rigaku Smartlab9KW diffraction system with a Cu $K\alpha$ source (λ = 1.54056 Å). XPS measurements were performed on Thermo ESCALAB 250XI, adopting Mg as the excitation source.

Electrocatalytic measurements: All electrochemical experiments were conducted using a CHI 660E electrochemical analyzer (CH Instruments, Inc., Shanghai). The electrochemical activity of the NiCoP foam/NF for HER and OER was performed with a three-electrode system. In this setup, the as-prepared NiCoP foam/NF served as the working electrode, a Hg/HgO electrode was employed as the reference electrode, and a graphite rod was utilized as the counter electrode. The overall water-splitting performance of the electrolyzers was tested in a two-electrode system, designating the OER electrode as the anode and the HER electrode as the cathode. The experiments were conducted in a strong alkaline seawater electrolyte, with a pH of approximately 14. To mitigate the influence of the Ni^{2+} to Ni^{3+} oxidation peak on the catalytic current density and ensure accurate overpotential calculations, linear sweep voltammetry (LSV) was performed using backward scans (from positive to negative direction) for the polarization curves. In this

study, the changing potentials were reported relative to the reversible hydrogen electrode (RHE), based on the following equation:

$$E(vs.RHE) = E(vs.Hg/HgO) + 0.059pH + 0.098V$$

Cyclic voltammetry (CV) curves for the OER were obtained within a potential range of 0 V to 1.5 V versus Hg/HgO, at a scan rate of 50 mV/s over 50 cycles to activate the electrodes. Similarly, CV curves for the HER were recorded from –2 V to 0 V versus Hg/HgO, also at a scan rate of 50 mV/s for 50 cycles. The LSV parameters for OER and HER were set with a scanning range of 1.5 V to 0 V, and –2 V to 0 V, respectively, both at a scan rate of 10 mV/s. The potential range of CV curves for overall water-splitting is from 3.2 V to 1.0 V, and the scan rate is 10 mV/s for 50 cycles. All tests were conducted at a controlled temperature of 25 ± 1 °C. The electrochemical impedance spectroscopy (EIS) measurements spanned a frequency range of 0.01 Hz to 100 kHz. To determine the double-layer capacitance (C_{dl}) values, CV curves were generated at varying scan rates from 30 ~ 90 mV/s. The chronopotentiometry stability test was carried out to assess the stability and durability of the catalysts under a constant high current density of 1000 mA/cm² for OER, HER, and overall water-splitting. All data have been adjusted for iR compensation. The iR-compensated potential was calculated based on the following equation:

$$E_{corr} = E - iR$$

where E is the original potential, R is the solution resistance, i is the corresponding current, and E_{corr} is the iR-compensated potential.

Gas Chromatography Test: Seawater oxidation for gas chromatography (Shimadzu GC-2014C TCD) tests were conducted in a sealed custom-built three-electrode cell containing

a 1 M KOH + seawater electrolyte. To sustain oxygen production, chronopotentiometry was employed, maintaining a steady current of 500 mA/cm^2.

Phosphate buffer solution (PBS, pH 6.5): Initially, 12 g of Na_2HPO_4 and 23 g of KH_2PO_4 were mixed into 100 mL of deionized water until fully dissolved. Following this, 100 mL of an EDTA-2Na aqueous solution (4 mg/mL) was incorporated into the mixture. This combined solution was then poured into a 500 mL volumetric flask and topped up with deionized water to the marked scale line.

DPD chromogenic agent: Firstly, 0.5 g of DPD was dissolved in 100 mL of deionized water containing 2 mL of concentrated H_2SO_4 and 0.1 g of EDTA-2Na. The mixture was then diluted to a total volume of 500 mL and transferred to a brown bottle, which should be stored away from light to maintain its stability.

Active chlorine standard curve: Since directly obtaining a standard solution of active chlorine is challenging, a widely used method involves employing $KMnO_4$ as an oxidizing agent to convert its oxidation capacity into an equivalent active chlorine content, thereby establishing the standard curve. Through practical calibration with a sodium hypochlorite solution, observing changes in oxidation states during the reaction, and measuring the absorbance of the reactants, it has been established that a solution of 891 mg/L $KMnO_4$ is equivalent to a 1000 mL/g chlorine-containing standard solution. This conversion forms the basis for establishing a standard curve for active chlorine using the masses of the mentioned substances.

Determination of active chlorine: The active chlorine concentration in the electrolyte was measured with the DPD method and a UV-vis spectrophotometer. (*J. Electroanal. Chem.*,

2018, **819**,260; *Inorg. Chem. Front.*, 2023, **10**, 2100) Initially, 100 µL of the electrolyte was sequentially combined with 50 µL of H_2SO_4 (1.0 M), 50 µL of NaOH (2.0 M), and 4.8 mL of deionized water. Subsequently, 250 µL of DPD reagent and 250 µL of PBS (pH = 6.5) were added to the mixture. After following the solution to stand for two minutes, it turned a transparent pink color. The absorbance at 550 nm was then recorded using UV-visible absorption spectroscopy to analyze the concentrations of various active chlorine species.
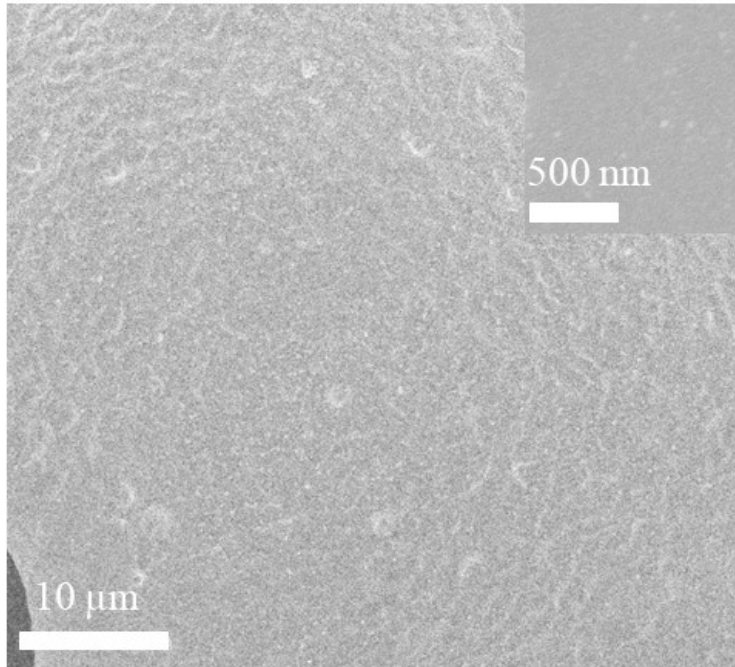
Fig. S1. SEM images of bare NF.
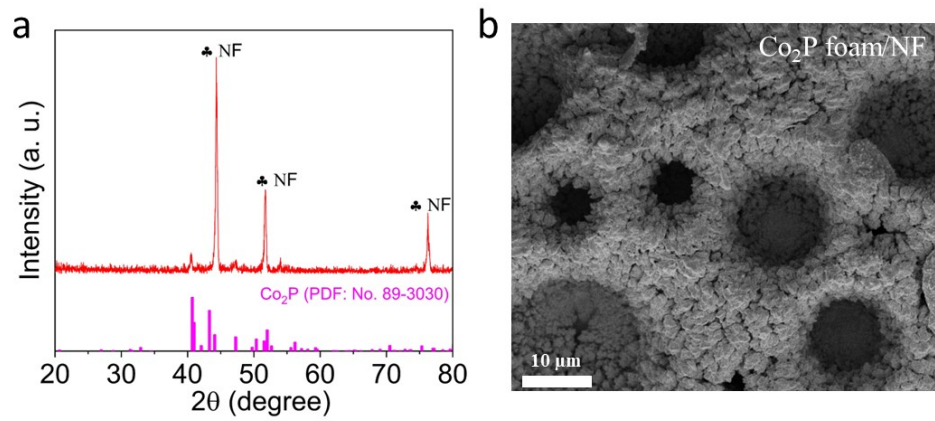
Fig. S2. (a) XRD pattern and (b) SEM image of Co_2P foam/NF.
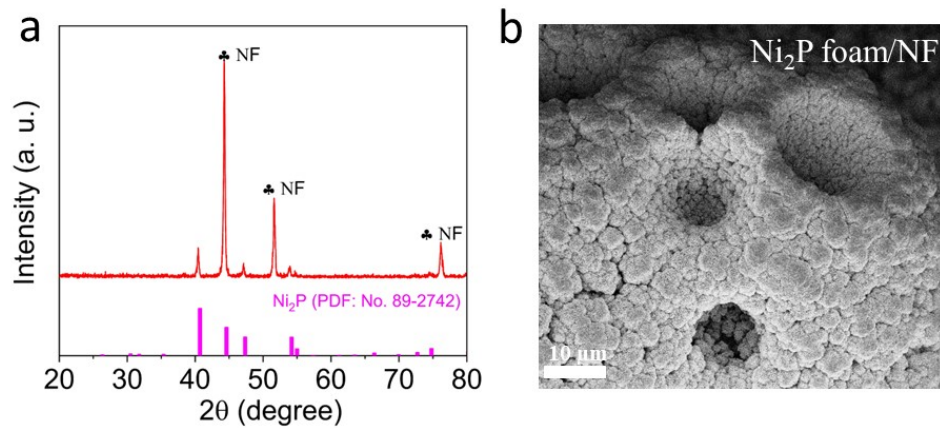
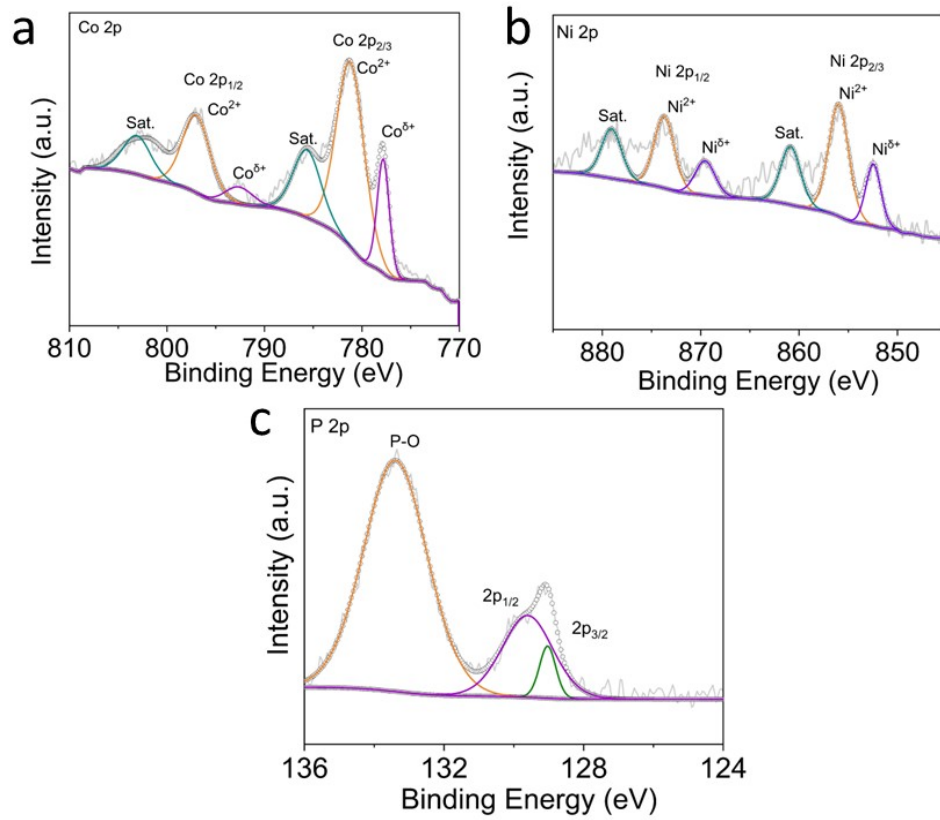**Fig. S3.** (a) XRD pattern and (b) SEM image of Ni$_2$P foam/NF.

Fig. S4. High-resolution XPS spectra for NiCoP in the (a) Co 2p, (b) Ni 2p, and (c) P 2p regions.
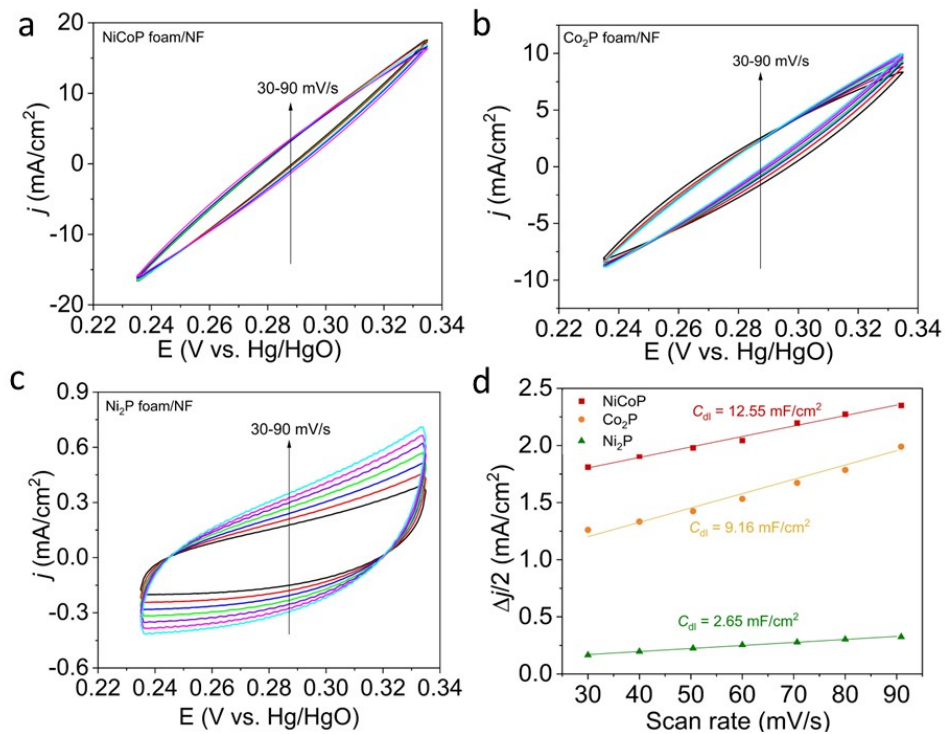
Fig. S5. Cyclic voltammetry curves for (a) NiCoP foam/NF, (b) Co_2P foam/NF, and (c) Ni_2P foam/NF in the double layer region at different scan rates of 30 ~ 90 mV/s. (d) Capacitive current densities of NiCoP foam/NF, Co_2P foam/NF, and Ni_2P foam/NF at 0.285 V vs. Hg/HgO as a function of the scan rate.
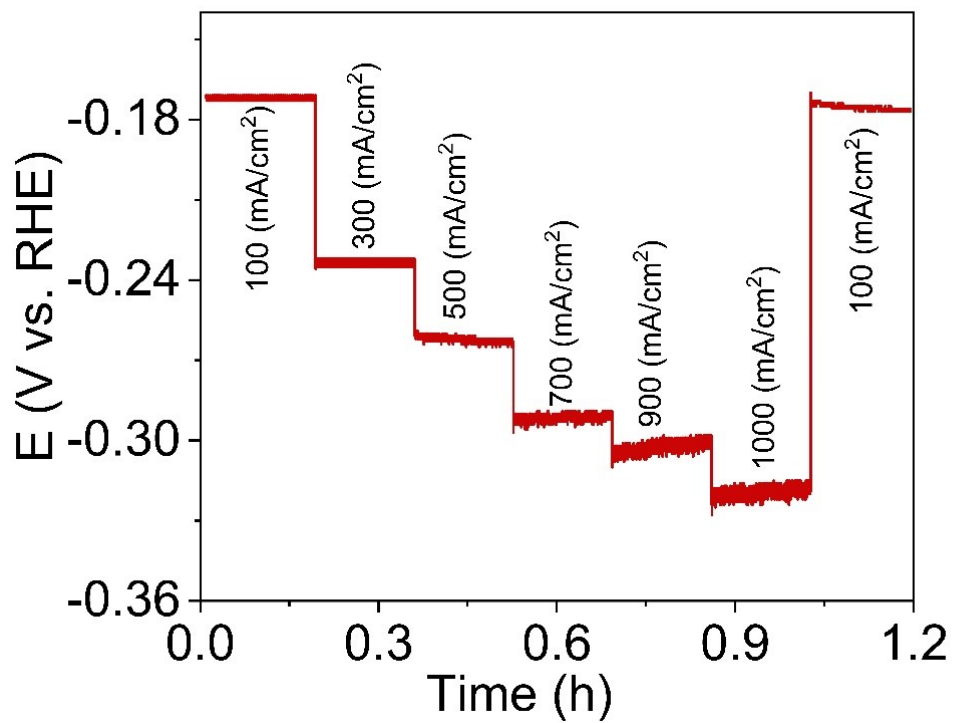
Fig. S6. Multi-current process of NiCoP foam/NF for HER. The current density started at 100 mA/cm^2 and ended at 100 mA/cm^2.
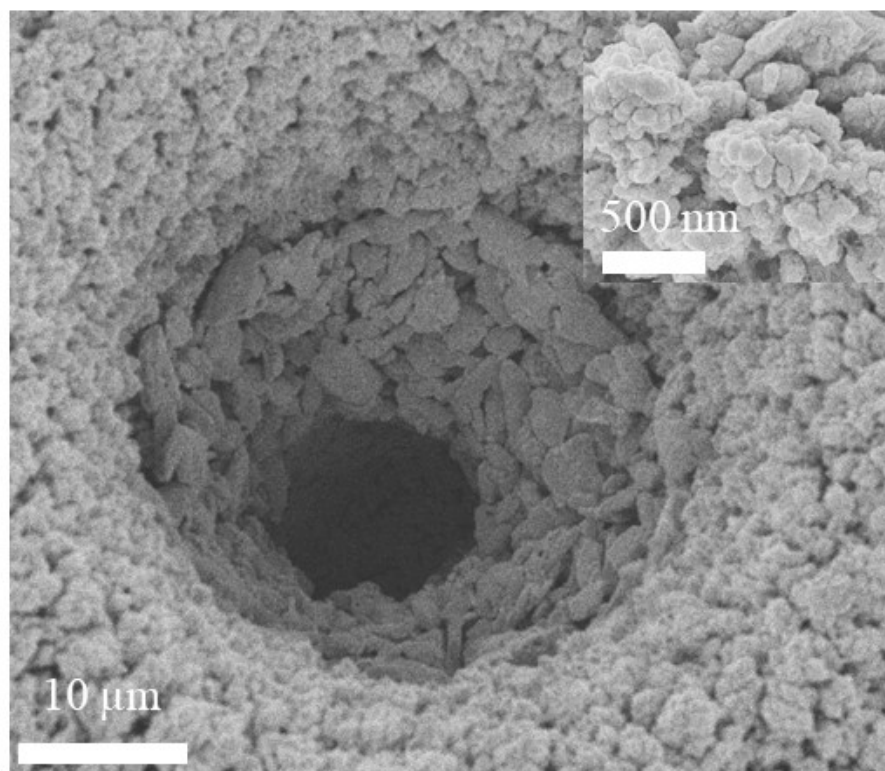
Fig. S7. SEM images of NiCoP foam/NF after durability test of HER in 1 M KOH + seawater solution.
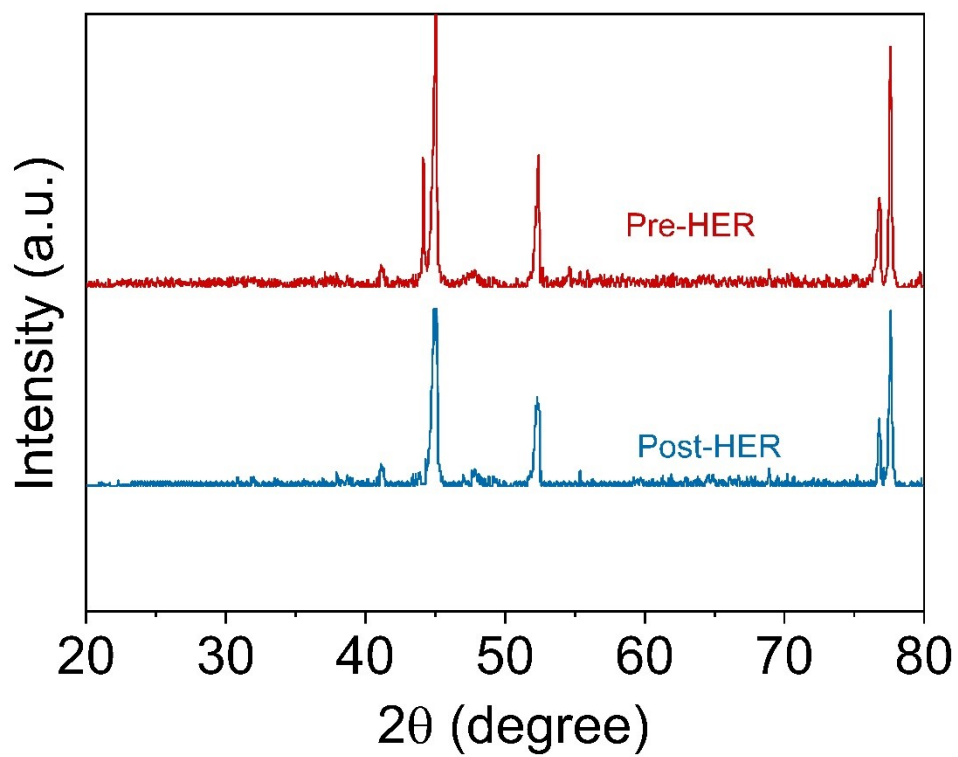
Fig. S8. XRD patterns for pre- and post-HER NiCoP foam/NF tested in 1 M KOH + seawater solution.

Fig. S9. Multi-current process of NiCoP foam/NF for OER. The current density started at 100 mA/cm^2 and ended at 100 mA/cm^2.

Fig. S10. (a) UV-vis absorption spectra of ClO⁻ with different concentrations. (b) Calibration curve used for calculating ClO⁻concentrations of the electrolyte.

Fig. S11. SEM images of NiCoP foam/NF after durability test of OER in 1 M KOH + seawater solution.

Fig. S12. XRD patterns for pre- and post-OER NiCoP foam/NF tested in 1 M KOH + seawater solution.
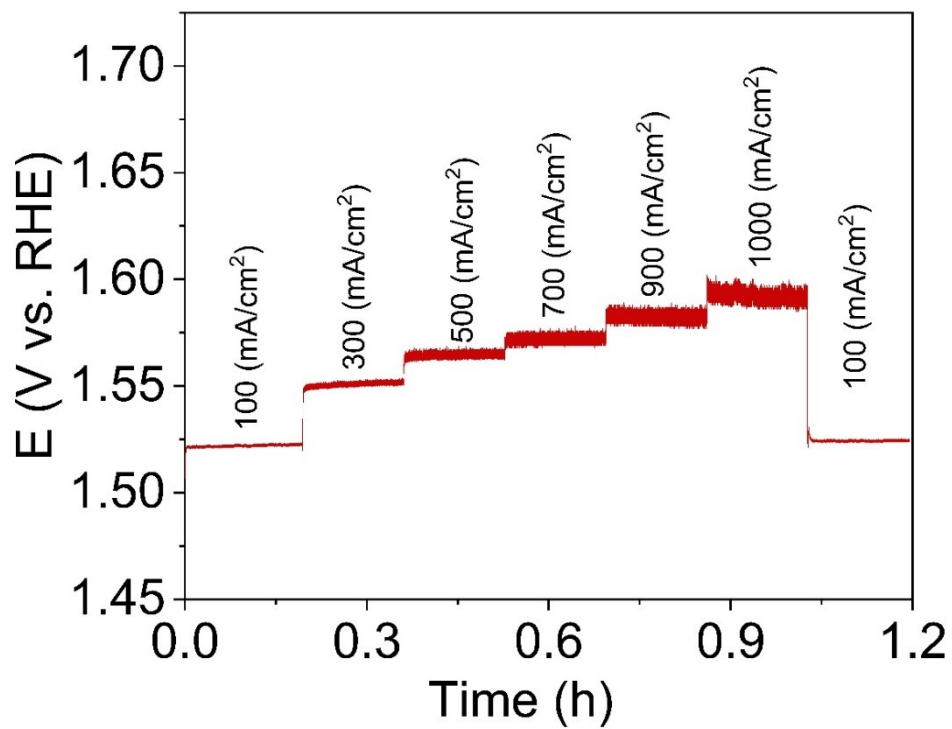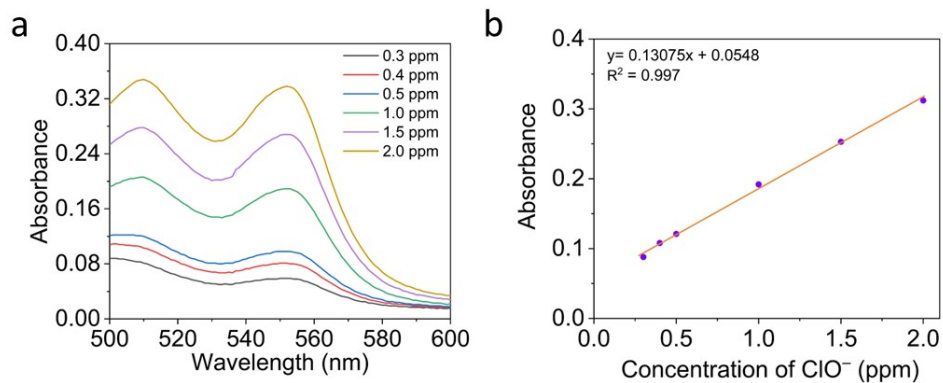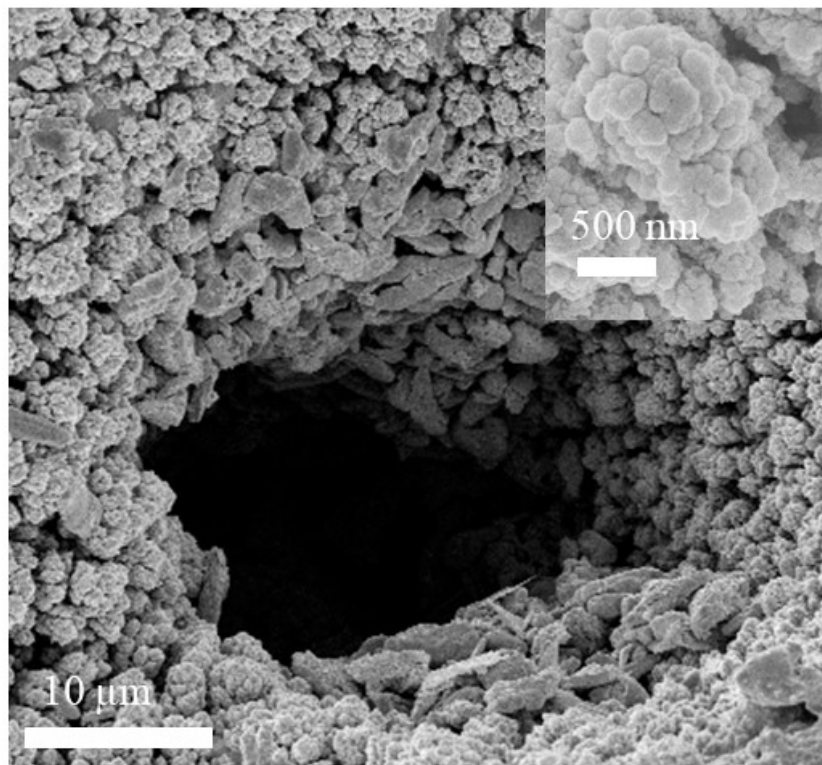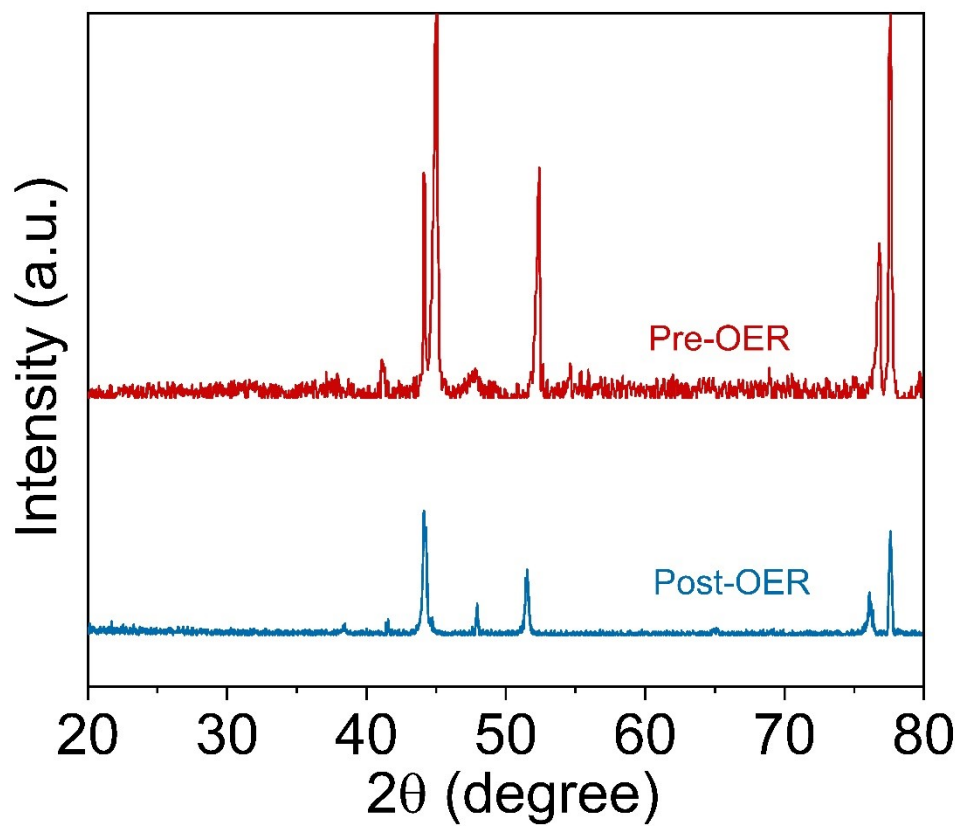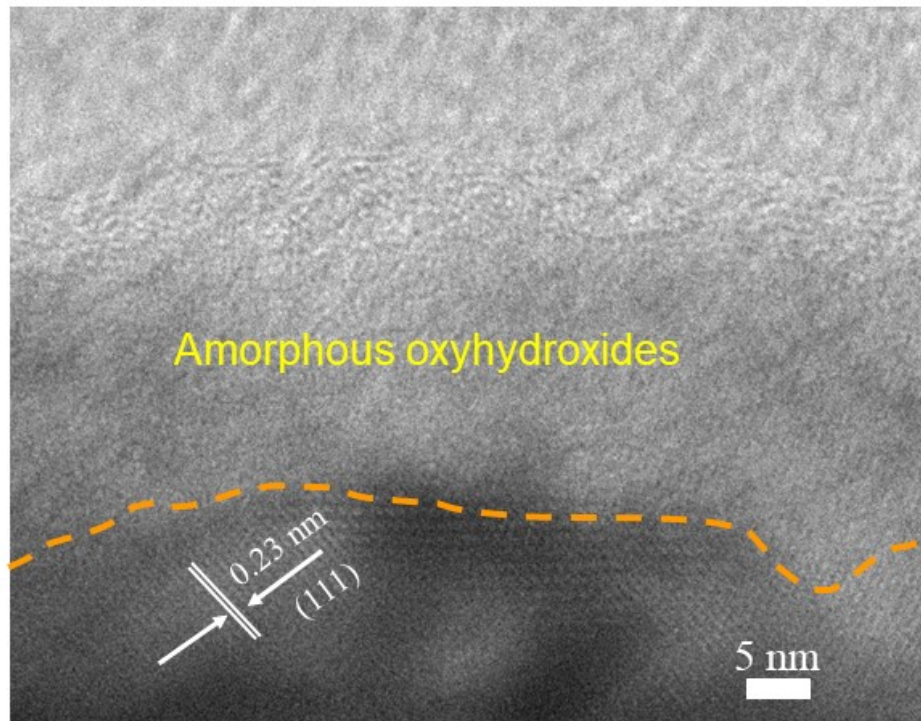
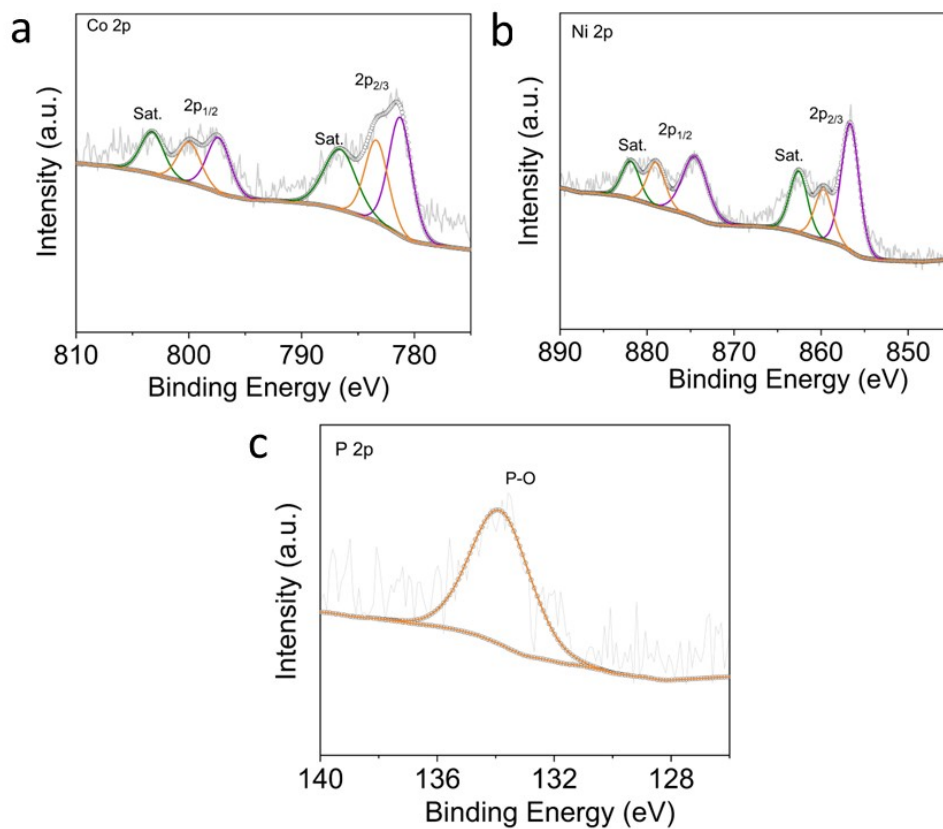**Fig. S13.** HRTEM image of NiCoP after durability test of OER in 1 M KOH + seawater solution.

Fig. S14. High-resolution XPS spectra for NiCoP in the (a) Co 2p, (b) Ni 2p, and (c) P 2p regions after durability test of OER in 1 M KOH + seawater solution.

Table S1. Comparison of HER performances for NiCoP foam/NF with recently reported electrocatalysts in alkaline seawater.

Electrocatalyst	Electrolyte	η_{100} (mV)	η_{1000} (mV)	Testing time	Ref.
NiCoP foam/NF	1 M KOH + seawater	171	328	300 h @1000 mA/cm^2	This work
B-NiCoP	1 M KOH + seawater	223	N/A	85 h @100 mA/cm^2	*ACS Appl. Energy Mater.*, 2023, **6**, 10713–10722
Fe$_2$P/Ni$_2$N	1 M KOH + seawater	109	208	40 h @100 mA/cm^2	*Small*, 2023, **19**, 2207082
Ru-CoO$_x$/NF	1 M KOH + seawater	120	252	100 h @70 mA/cm^2	*Small*, 2021, **17**, 2102777
Co$_x$P$_v$@NF	1 M KOH + seawater	189	232	100 h @800 mA/cm^2	*Nano Energy*, 2023, **109**, 108292
MnCo/NiSe/NF	1 M KOH + seawater	202	270	200 h @500 mA/cm^2	*Appl. Catal. B*, 2023, **325**, 122355
Ni$_2$P-Fe$_2$P/NF	1 M KOH + seawater	232	389	40 h @500 mA/cm^2	*Adv. Funct. Mater.*, 2021, **31**, 2006484
Co-P@NN	1 M KOH + seawater	245	365	N/A	*J. Colloid Interface. Sci.*, 2023, **645**, 227–240
Ru-Ni(Fe)P$_2$/NF	1 M KOH + seawater	280	361	N/A	*Small*, 2023, **19**, 2300030
Mn-doped Ni$_2$P/Fe$_2$P	1 M KOH + seawater	300	470	100 h @500 mA/cm^2	*Chem. Eng. J.*, 2023, **454**, 140061
RuNi-Fe$_2$O$_3$/IF	1 M KOH + seawater	150	350	20 h @100 mA/cm^2	*Chinese J. Catal.*, 2022, **43**, 2202–2211

η_{100} represents the overpotentials required to attain *j* of 100 mA/cm^2.

η_{1000} represents the overpotentials required to attain j of 1000 mA/cm^2.

Table S2. Comparison of OER performances for NiCoP foam/NF with other reported electrocatalysts in alkaline seawater.

Electrocatalyst	Electrolyte	η_{100} (mV)	η_{1000} (mV)	Testing time	Ref.
NiCoP foam/NF	1 M KOH + seawater	291	356	300 h @1000 mA/cm^2	This work
Fe$_2$P-NiCoP	1 M KOH + seawater	300	N/A	30 h @20 mA/cm^2	*Mater. Today Physics,* 2022, **24**, 100684
Fe$_2$P/Ni$_2$N	1 M KOH + seawater	225	340	40 h @500 mA/cm^2	*Small,* 2023, **19**, 2207082
Co$_x$P$_v$@NF	1 M KOH + seawater	287	356	N/A	*Nano Energy*, 2023, **109**, 108292
Mn-doped Ni$_2$P/Fe$_2$P	1 M KOH + seawater	240	358	100 h @500 mA/cm^2	*Chem. Eng. J.,* 2023, **454**, 140061
Ru-CoO$_x$/NF	1M KOH + seawater	220	390	100 h @70 mA/cm^2	*Small,* 2021, **17**, 2102777
Ni$_2$P-Fe$_2$P/NF	1 M KOH + seawater	220	400	48 h @500 mA/cm^2	*Adv. Funct. Mater.,* 2021, **31**, 2006484
Co-P@NN	1 M KOH + seawater	389	435	24 h @10 mA/cm^2	*J. Colloid Interface. Sci.,* 2023, **645**, 227–240
MnCo/NiSe/NF	1 M KOH + seawater	N/A	460	100 h @70 mA/cm^2	*Appl. Catal. B,* 2023, **325**, 122355
Ru-Ni(Fe)P$_2$/NF	1 M KOH + seawater	287	520	N/A	*Small,* 2023, **19**, 2300030
RuNi-Fe$_2$O$_3$/IF	1 M KOH + seawater	330	495	20 h @100 mA/cm^2	*Chinese J. Catal.,* 2022, **43**, 2202–2211

Table S3. Comparison of overall seawater splitting performance of NiCoP foam/NF ‖ NiCoP foam/NF with recently reported electrocatalysts under alkaline conditions.

Electrocatalyst	Electrolyte	V_{100} (V)	V_{1000} (V)	Testing time	Ref.
NiCoP foam/NF ‖ NiCoP foam/NF	1 M KOH + seawater	1.28	1.97	300 h @1000 mA/cm^2	This work
Fe$_2$P/Ni$_2$N ‖ Fe$_2$P/Ni$_2$N	1 M KOH + seawater	1.65	N/A	40 h @500 mA/cm^2	*Small*, 2023, **19**, 2207082
Co$_x$P$_v$@NF ‖ Co$_x$P$_v$@NF	1M KOH + seawater	1.54	1.88	N/A	*Nano Energy*, 2023, **109**, 108292
Mn-Ni$_2$P/Fe$_2$P ‖ Mn-Ni$_2$P/Fe$_2$P	1 M KOH + seawater	1.82	N/A	120 h @500 mA/cm^2	*Chem. Eng. J.*, 2023, **454**, 140061
Ru-CoO$_x$/NF ‖ Ru-CoO$_x$/NF	1 M KOH + seawater	1.55	2.62	N/A	*Small*, 2021, **17**, 2102777
Ni$_2$P-Fe$_2$P/NF ‖ Ni$_2$P-Fe$_2$P/NF	1 M KOH + seawater	1.87	2.1	N/A	*Adv. Funct. Mater.*, 2021, **31**, 2006484
Co-P@NN ‖ Co-P@NN	1 M KOH + seawater	1.82	2.2	N/A	*J. Colloid Interface. Sci.*, 2023, **645**, 227–240
MnCo/NiSe/NF ‖ MnCo/NiSe/NF	1 M KOH + seawater	N/A	3.03	200 h @500 mA/cm^2	*Appl. Catal. B*, 2023, **325**, 122355
Ru-Ni (Fe)P$_2$/NF ‖ Ru-Ni (Fe)P$_2$/NF	1 M KOH + seawater	N/A	2.59	50 h @600 mA/cm^2	*Small*, 2023, **19**, 2300030
RuNi-Fe$_2$O$_3$/IF ‖ RuNi-Fe$_2$O$_3$/IF	1 M KOH + seawater	2.8	3.12	100 h @100 mA/cm^2	*Chinese J. Catal.*, 2022, **43**, 2202–2211